

## Floquet description of multiphoton processes in Li

D. I. Duncan, J. G. Story, and T. F. Gallagher

*Department of Physics, University of Virginia, Charlottesville, Virginia 22901*

(Received 20 March 1995)

We have made several different types of measurements of the three-photon ionization of Li produced by 3-ps laser pulses and describe the results using a Floquet picture. Over the photon frequency range 15 000 to 15 800  $\text{cm}^{-1}$ , Li represents a strongly coupled three-state system with the  $2s$  ground state coupled to the  $2p$  and  $3d$  states by one and two photons, respectively. Energy analysis of the photoelectrons allows the measurement of the intensity dependent shift of the  $2s$  Floquet state during the laser pulse. The shift shows a strong frequency dependence that is not predicted by first-order perturbation theory. We have also measured the total ionization spectrum over several ranges of frequency, as well as the angular distribution of the ionization and the first above-threshold ionization peak for frequencies where the ground state is near resonance with the  $4s$  and  $4d$  excited states. Calculations based on the Floquet Hamiltonian indicate that all of these processes may be understood in terms of a Floquet description.

PACS number(s): 32.80.Rm

### I. INTRODUCTION

It has recently been shown that ionization of atoms with short intense laser pulses can be understood in terms of a Floquet description [1–5]. In particular, Floquet theory has proven to be very useful in describing the evolution of bound intermediate states during the laser pulse, which, in turn, is critical to understanding the ionization process. Floquet analysis offers a view of the multiphoton ionization process in which the atomic states evolve with the field, and it has the following advantages. First, it removes the rapid time variation at the optical frequency by transforming the time-dependent Hamiltonian of an atom interacting with an oscillating laser field into an equivalent time-independent Floquet Hamiltonian. By taking the relatively slow variation of the laser field amplitude into account, it is rather simple to calculate the time evolution of the Floquet states by diagonalizing the Floquet Hamiltonian for successive values of the field amplitude during the laser pulse. Second, the Floquet model incorporates effects that cannot be anticipated from lowest-order perturbation theory.

In this paper we present the results of a variety of measurements taken for the multiphoton ionization of Li. Specifically, we have measured the three-photon ionization spectrum, the shift of the ground state, and angular distributions of electrons ejected in both the ionization and first above-threshold ionization (ATI) peaks. We show that a very simple Floquet model, which is essentially a dressed-state representation of atomic levels in the presence of a strong laser field, can be used to explain all of these measurements.

### II. THEORY

In the Floquet picture, integral multiples of the photon energy are added to or subtracted from the atomic energy levels so that all Floquet states lie in an energy range spanned by the photon energy. The eigenvectors of the

Floquet Hamiltonian are the adiabatic Floquet or dressed states of the atom, and the eigenvalues are their corresponding quasienergies. Specifically, the Floquet states are linear combinations of atomic states coupled by the field, while the quasienergy includes the ac Stark shift of the atomic state. The Floquet states evolve with the field, and this evolution can either be adiabatic, diabatic, or a mixture of both. If the evolution is partially diabatic, the initial Floquet state is projected onto another Floquet state. This situation is possible near zero field, when nearby Floquet states interact and shift away from each other, or at the full avoided crossings, which occur when a state is ac Stark shifted into resonance during the laser pulse. The evolution of a state through a level crossing can be described by the two-level Landau-Zener theory [6,7] and depends on the relative sizes of the squared magnitude of the avoided crossing and the rate of change of the energy difference between the two levels.

It is interesting to consider the ionization of Li with photons having a wavelength near 650 nm. At these frequencies, not only is the ground state near resonance with the  $2p$  and  $3d$  states with one and two photons, respectively, but the  $2s$ - $2p$  and  $2p$ - $3d$  oscillator strengths are nearly equal (0.753 and 0.667, respectively), resulting in a strongly coupled three-level system. Figure 1 shows an energy-level diagram of Li with photons having  $\lambda$  near 650 nm, as well as the zero-field Floquet levels over the range of laser frequencies for which the  $2s$ ,  $2p$ , and  $3d$  states are strongly coupled. The ground Floquet state is defined to have zero energy; one photon energy was subtracted from the  $2p$  energy to obtain the  $2p$  Floquet state, and twice the photon energy was subtracted from the  $3d$  state to obtain the  $3d$  Floquet state.

To gain insight into the ionization process, we would like to know how the Floquet levels evolve as the laser pulse turns on. This evolution can be calculated by diagonalizing the Floquet Hamiltonian according to the method of Shirley [8]. In principle, this Floquet Hamiltonian is an infinite matrix and includes the atom interac-

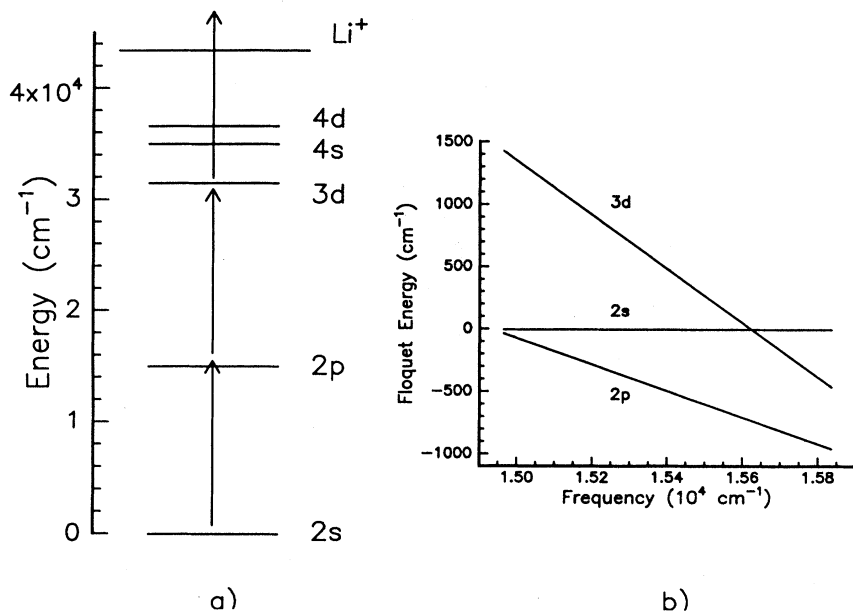


FIG. 1. (a) Energy-level diagram showing the intermediate atomic energy levels relevant to this experiment. Photons having  $\lambda$  near 650 nm are represented by arrows, which also show how the ground state is near resonance with the 2p and 3d states with one and two photons, respectively. (b) The zero-field Floquet energy levels as a function of laser frequency over the frequency range for which Li is a strongly coupled three-level system.

tion with the laser field to all orders. In practice, one can always reduce the problem to diagonalizing a finite submatrix. For the range of frequencies and intensities in our experiment, we find that the Floquet matrix simplifies in the following two ways. First, only a single Floquet block is needed. As long as the energy shift of the Floquet levels during the laser pulse is small compared to the photon energy, one Floquet block is all that is needed to provide a convergent result. Second, the Floquet matrix contains only three states, namely the ground, 2p, and 3d Floquet states. Adding to the matrix, the nearest Floquet states that could be coupled to the 2p state by the laser field—the 3s, 4s, and 4d states—did not appreciably change the results. We then arrive at the conclusion that calculating the evolution of the relevant Floquet states in the ionization of Li by photons having a wavelength of nearly 650 nm is accomplished very simply by diagonalizing the following  $3 \times 3$  matrix:

$$\begin{bmatrix} E_{2s} & \mu_{2s-2p} & 0 \\ \mu_{2s-2p} & E_{2p} - \omega & \mu_{2p-3d} \\ 0 & \mu_{2p-3d} & E_{3d} - 2\omega \end{bmatrix}$$

where the  $E$ 's are zero-field atomic level energies and the  $\mu$ 's are dipole matrix elements.

Diagonalization of the Floquet matrix yields information about the ionization process in two ways. The eigenvectors show how the zero-field atomic states acquire the state character of those states to which they are coupled by the laser field, and the eigenvalues give the ac Stark shift of the atomic states. The calculation of state character is used in a simple Floquet model proposed by Papiannou and Gallagher [1] to describe ionization in the following way. When the laser pulse turns on, the Floquet ground state wave function may be written as

$$\Psi_g = \sum a_n \Phi_n, \quad (1)$$

where the  $\Phi_n$ 's are the zero-field Floquet states to which the ground state is coupled by the laser field, and the  $a_n$ 's give the excited-state character fractions of the ground Floquet state, with  $\sum a_n^2 = 1$ . For purely adiabatic evolution, as is the case in this experiment, ionization occurs by the ionization of the excited-state fraction of the ground Floquet state, where an excited state is understood to be one that is bound by less than one photon energy. The ionization rate can be written

$$\Gamma_g = \sum \Phi \sigma_n |a_n|^2, \quad (2)$$

where  $\Phi$  is the photon flux and  $\sigma_n$  is the one-photon ionization cross section of the  $n$ th excited state. Since the ionization rate varies nonlinearly with intensity, ionization occurs approximately at the field for which the ionization rate equals half the inverse laser pulse length.

The results of diagonalizing the Floquet Hamiltonian for several different laser frequencies are shown in Fig. 2. Plotted in the figure is the character composition of the ground Floquet state (i.e.,  $|a_n|^2$  for each of its character fractions) as a function of intensity, while the inset shows the shift in energy of the ground, 2p, and 3d Floquet states over the same range of intensity. The results of Fig. 2 show that how a state shifts in energy indicates how it acquires state character. For example, in Fig. 2(a) a frequency of  $15060 \text{ cm}^{-1}$  (664 nm) locates the ground state  $157 \text{ cm}^{-1}$  above the 2p state and  $1162 \text{ cm}^{-1}$  below the 3d state at zero field. As the laser pulse turns on, the strong 2s-2p coupling causes the ground state to adiabatically move upward in energy and the Floquet ground state becomes a mixture of the 2s and 2p states. This situation is reflected in the state character plot at low intensities as a sudden increase in 2p character with a corresponding decrease in 2s character. As the ground state continues to shift upward at higher intensities, the 2p

fraction of its character interacts with the  $3d$  state and, correspondingly, the ground Floquet state acquires  $3d$  character at the expense of its  $2p$  character. The coupling to the  $3d$  state counteracts the coupling to the  $2p$  state, pushing the ground state downwards in energy, which can be seen as a leveling off of the ground Floquet state energy at higher intensities. Similar arguments can be used to explain the plots of Fig. 2(b), which were calculated for a laser frequency that places the ground Floquet state above both the  $2p$  and  $3d$  states at zero field. The results for a laser frequency that makes the ground and  $3d$  Floquet state degenerate at zero field [Fig. 2(c)] are drastically different from the previous two cases. The  $2p$  character of the ground Floquet state has completely

disappeared, and the ground Floquet energy level remains flat for all intensities. The disappearance of the  $2p$  character of the ground Floquet state can be interpreted as light-induced structure. If the laser was considered a dressing field, a second probe laser would locate a dark resonance when used to determine the effects of this dressing field (an attempt to detect the dark  $2p$  resonance in this experiment was unsuccessful). The fact that the ground Floquet state does not shift in energy as a function of intensity at this laser frequency is a nonperturbative result and is a manifestation of Li being a strongly coupled three-level system.

It is interesting to examine the behavior of the shift of the ground Floquet state in the insets of Fig. 3 in greater

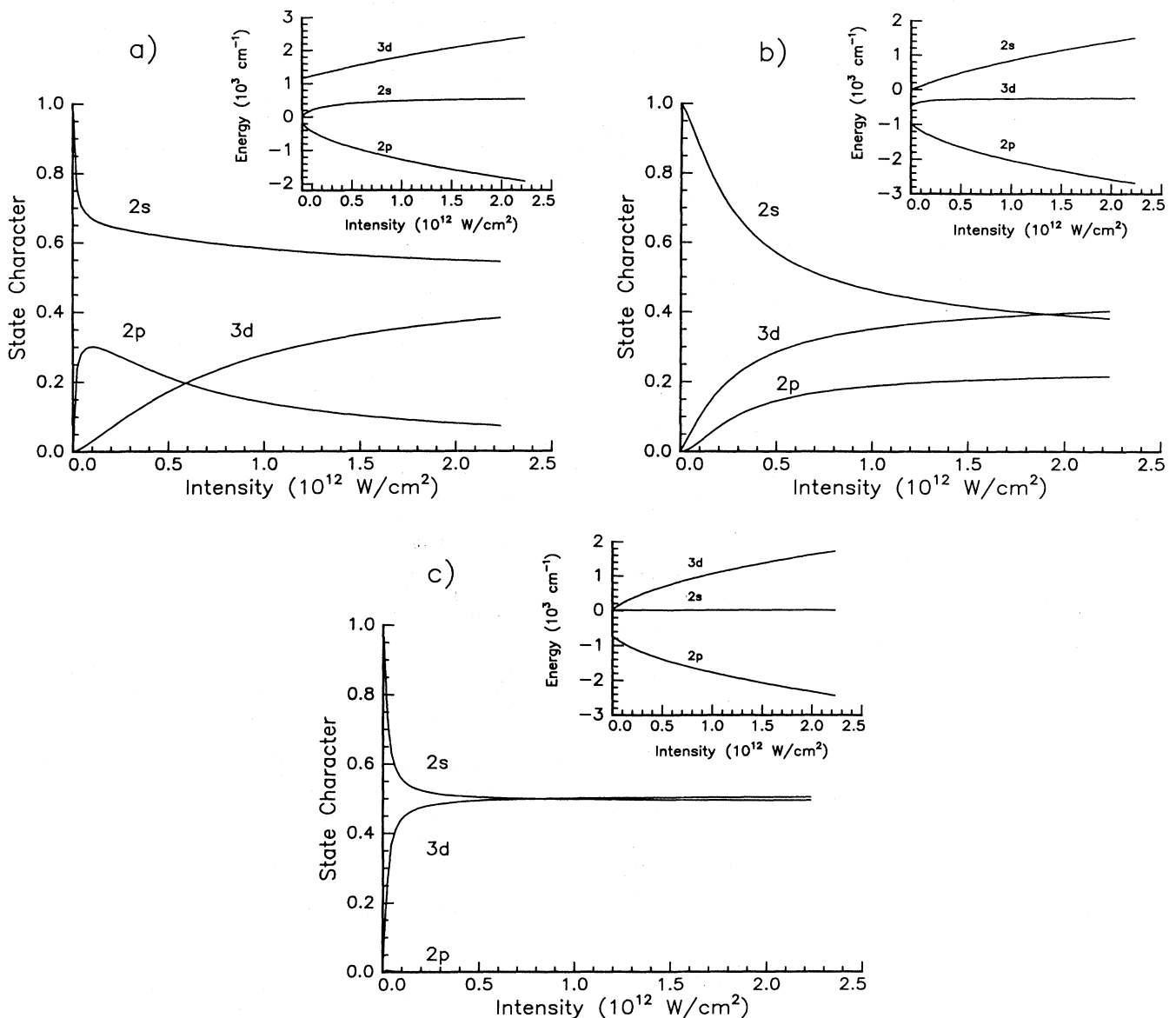


FIG. 2. (a) State character of the adiabatic ground Floquet state as a function of laser intensity for  $\lambda = 664$  nm. The inset shows the Floquet energy levels over the same range of intensity where the Floquet levels are labeled by the zero-field state to which they adiabatically connect. (b) same as in (a) for  $\lambda = 630$  nm. (c) same as in (a) for  $\lambda = 639$  nm.

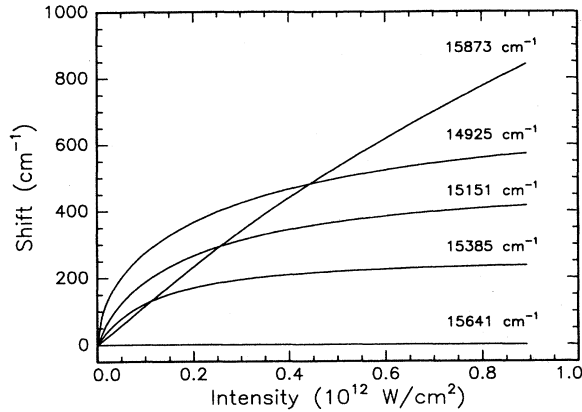


FIG. 3. Shift in energy of the ground Floquet state as a function of laser intensity for several different laser frequencies. A laser frequency of  $15\,641\text{ cm}^{-1}$  makes the ground state plus two photons resonant with the  $3d$  state.

detail. It is clearly dependent on the laser frequency, or equivalently, the relative positions of the ground,  $2p$ , and  $3d$  Floquet states. Figure 3 shows the results of calculations of the ground-state shift as a function of intensity for several laser frequencies. For the lowest frequency of the experiment ( $14\,925\text{ cm}^{-1}$ ), the ground Floquet state lies just above the  $2p$  Floquet state and it experiences a sharp initial upward shift towards the  $3d$  state. At higher intensities, the coupling with the  $3d$  state counteracts this upward shift and the shift of the ground state levels off. For higher frequencies, the interaction with the  $3d$  state occurs at lower intensities. As a result, the shift of the ground state levels off at lower intensities until it is zero when the ground and  $3d$  Floquet states are degenerate. At frequencies where the ground state lies above both the  $2p$  and  $3d$  Floquet states, the couplings to the  $2p$  and  $3d$  states both push the ground Floquet state upwards in energy—the shift of the ground state continues to rise with increasing intensity. First-order perturbation theory does not predict this behavior, but we see that it is readily apparent in a simple Floquet analysis. We describe the experimental verification of this behavior of the ground-state shift, as well as other measurements that can be explained with a Floquet model, in the following sections.

### III. EXPERIMENT

The experiment was performed by exciting Li atoms in an effusive atomic beam with a focused picosecond dye laser. An actively mode-locked Antares neodymium-doped yttrium aluminum garnet (Nd:YAG) laser was used to pump a synchronously mode-locked Coherent 700 tunable dye laser producing pulses 3 ps in length. A Nd:YAG regenerative amplifier was used to pump a four-stage Bethune cell dye amplifier, giving final pulse energies between 0.25 and 0.8 mJ depending on the dye being used. It was important to minimize the amount of amplified spontaneous emission (ASE) present in the final pulse, which was always less than 15%, as the  $2p$  and  $3d$  states are easily populated by ASE. The beam waist was measured by moving a razor blade across the beam at the

focus and monitoring the transmitted intensity with a photodiode. The result gave a beam waist of approximately  $60\text{ }\mu\text{m}$ , which, for a pulse energy of 0.25 mJ, gives a maximum laser intensity at the focus of  $7 \times 10^{11}\text{ W/cm}^2$ . For the measurement of the total ionization spectra, the laser and atomic beams intersected one another between two field plates spaced 1 cm apart defining the interaction region. A high-voltage pulse was applied to the bottom plate approximately 350 ns after the firing of the laser, driving all ions produced by ionization up through a mesh-covered hole in the upper field plate to a set of microchannel plates, where they were detected. A gated integrator recorded the ion spectrum while the frequency of the laser was scanned, and a photodiode was used to simultaneously monitor the laser intensity. To measure the shift of the ground state, the field plate assembly was replaced by a time-of-flight electron spectrometer, which could detect electrons with energies as low as 100 meV. The spectrometer consisted of a copper tube 24 cm in length and 10 cm in diam. The top end of the tube was capped with a copper cap. Photoelectrons excited the flight tube through a copper mesh-covered 2.5-cm-diam hole and were subsequently detected by a microchannel plate assembly mounted directly over the hole. The flight tube assembly was grounded and placed inside a  $\mu$ -metal container to shield the interaction region and electron flight path from any stray magnetic fields. The largest magnetic field measured along the electron flight path was 20 mG, less than a few percent of the earth's field.

The laser and atomic beam entered the electron spectrometer approximately 16.9 cm down from the top of the tube through small holes drilled in the side of the  $\mu$ -metal shield and copper flight tube. The input of the atomic beam was apertured by a pinhole with the exit hole being much larger to prevent any accumulation of metal on the inside of the flight tube. The laser and atomic beams intersected each other at right angles in the center of the tube, with the polarization of the laser being linear and parallel to the vertical axis of the flight tube. The electron spectrometer was calibrated for each data set taken. This was done by using neutral density filters to attenuate the laser to 8% of its maximum intensity and recording the resulting electron spectra for steps of 2 nm over the range of laser frequency used in the experiment. Electron spectra resulting from full laser intensity were also obtained at each frequency, and a photodiode recorded the laser intensity. The electron peaks resulting from ionization of the ground state with low laser intensity have negligible ac Stark shifts, and their energies should be given by  $3h\nu - \text{IP}$ , where IP is the ionization potential of Li. These calibration peaks were fit to a time-of-flight equation of the form

$$E = (a)^2 / (t - c)^2 + b, \quad (3)$$

where  $E$  is energy in electron volts and  $t$  is time in nanoseconds. The constant  $a$  is the time it takes for a 1-eV electron to travel 16.9 cm up the flight tube,  $b$  is an energy offset, and  $c$  is the time at which the laser fired. With  $c$  being a known quantity (84 ns),  $a$  and  $b$  were varied to best fit the calibration peaks. An almost exact

fit could be found for each data set using values of  $a$  between 285 and 300 ns and values of  $b$  between 0.02 and 0.05 eV. One can calculate  $a$  to be 285 ns, and an energy offset of  $b = 0.023$  eV corresponds to an uncertainty in the distance the electron travels of 0.2 cm. Once a calibration curve was found, the experimental electron peaks for both low and high laser intensity could be converted from time to energy and the relative energy shift between the two determined.

One other type of measurement was performed in this experiment. The angular distribution of the ionized photoelectrons was recorded by passing the laser beam through a double Fresnel rhomb that was slowly rotated by a motor. As a result of rotating the Fresnel rhomb, the laser polarization was rotated about an axis perpendicular to the vertical axis of the flight tube. A gated integrator the ionization signal while the laser polarization was rotated.

#### IV. RESULTS AND DISCUSSION

##### A. The total ionization spectra

According to the model of multiphoton ionization discussed earlier, calculating how the Floquet ground state acquires excited-state character determines the total ionization. We have recorded the ionization spectrum as a function of laser frequency for a range of frequencies that bring the ground state into resonance with several different excited states. As a function of frequency, the total ionization spectrum will usually follow the dye gain curve of the ionizing laser away from any strong intermediate resonances. Departures from this behavior indicate a strong coupling to an intermediate state and are, in fact, a reflection of how the Floquet ground state acquires state character.

The top trace in Fig. 4(a) shows the measured ionization spectrum over a frequency range that includes the ground state being resonant with the  $2p$  state at  $14903\text{ cm}^{-1}$  and with the  $3d$  state at  $15641\text{ cm}^{-1}$ , while the dotted trace shows the dye gain curve of the ionizing laser. The intensity is high enough so that the ionization is saturated at the  $3d$  resonance; this allows us to examine what the spectrum looks like in the wings of the resonance. We have also been careful to minimize the effects of ASE. By energy analyzing the ionized electrons, one can distinguish ionization peaks due to the absorption of a combination of ASE and laser photons from peaks due to laser photons only because the peaks will be at different energies. We found that when the ASE was less than 15% of the laser light (measured by blocking the seed beam into the dye amplifier and monitoring the output light with a photodiode) and a spatial filter was used to block parts of the beam having large amounts of ASE, the ionization peaks due to ASE disappeared. We therefore kept the ASE levels below 15% for all the measurements taken in this experiment and used a spatial filter if a portion of the beam contained large amounts of ASE. Fig. 4(b) shows a calculation of the ionization spectrum over the same range of laser frequency. Using the experimental laser intensity profile shown in the bottom trace

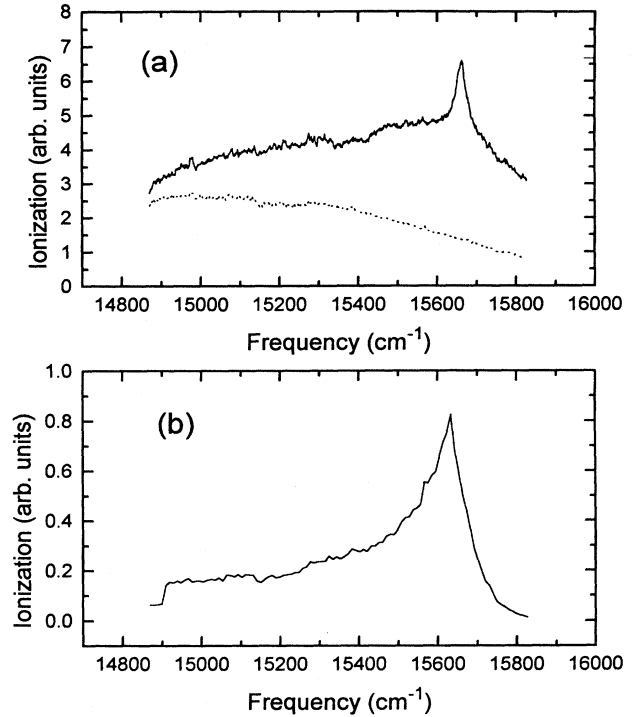


FIG. 4. (a) Top trace is the total ionization signal as a function of laser frequency. The ground state is resonant with the  $2p$  and  $3d$  states at laser frequencies of  $14903\text{ cm}^{-1}$  and  $15641\text{ cm}^{-1}$ , respectively. The dotted trace is the dye gain curve of the ionizing laser. (b) A single intensity (no spatial averaging) calculation of the total ionization signal over the same range of laser frequency as (a). Note that the  $2p$  resonance is characterized by a step in the ionization signal.

of Fig. 4(a) to determine couplings as a function of frequency, the Floquet Hamiltonian was diagonalized for steps of  $1\text{ cm}^{-1}$  and the amount of  $3d$  character that the Floquet ground state acquired was computed. The total ionization at a particular frequency is then proportional to the quantity

$$(\text{ionization}) \propto I * |a_{3d}|^2 \quad (4)$$

where  $I$  is the laser intensity and  $a_{3d}$  is the  $3d$  fraction of the ground Floquet state. Therefore, the plot in Fig. 4(b) gives the ionization at the peak laser intensity as a function of frequency. It is interesting to examine the behavior of the ionization spectrum near the  $2p$  and  $3d$  resonances in the calculation of Fig. 4(b). The  $2p$  resonance at  $14903\text{ cm}^{-1}$  is characterized by a step in the ionization signal; apparently, the ionization depends on whether the ground Floquet state is on the high- or low-energy side of the  $2p$  Floquet states. The Floquet model explains this behavior in the following way. In the first case, the ground Floquet state shifts *towards* the  $3d$  Floquet state, allowing it to acquire more  $3d$  character than in the second case, where it shifts *away* from the  $3d$  Floquet state. The ionization in Fig. 4(b) also depends on whether the ground Floquet state is on the high- or low-energy side of the  $3d$  Floquet state. On the low-energy side, the ionization spectrum gradually increases as a

function of laser frequency as the ground Floquet state is able to shift closer to the  $3d$  Floquet state acquiring more  $3d$  character. On the high-energy side, the ionization spectrum drops off sharply as the ground Floquet state shifts away from the  $3d$  Floquet state.

In the experimental spectrum of Fig. 4(a), the asymmetry around the  $3d$  resonance is clearly seen. On the low-energy side of the resonance, the ionization spectrum slowly increases as a function of frequency, even though the laser intensity is falling, while on the high-energy side the signal drops off sharply. However, there is no sign of any structure at  $14903\text{ cm}^{-1}$ , the  $2p$  resonance. The explanation for this absence of structure is found by taking into account the spatially varying intensity profile of a focused laser beam. The peak laser intensity is found at the center of the focus, with the intensity falling to zero at the edges of the focus. Calculations done for intensities lower than the peak intensity show that the amount of  $3d$  character acquired by the ground Floquet state does not heavily depend on whether the ground state is above or below the  $2p$  state. In other words, in the low-intensity regions of the focus, ionization near a laser frequency of  $14903\text{ cm}^{-1}$  occurs at an intensity such that the shift of the ground state is small compared to the energy difference between the ground and  $3d$  Floquet states. As a result, the ground Floquet state acquires the same amount of  $3d$  character whether it shifts towards or away from the  $3d$  Floquet state. Correspondingly, the step

seen in the ionization calculation of Fig. 4(b) is averaged away if the spatially varying intensity of the focus is taken into account.

The asymmetric behavior of the ionization spectrum near an excited-state resonance can be seen more clearly by tuning the laser frequency in the vicinity of the  $4s$  and  $4d$  excited states (see Fig. 1). The bottom trace in Fig. 5(a) shows the ionization spectrum as the frequency is scanned through resonance with the  $4s$  state, while the dotted trace is the dye gain curve of the laser. Since the coupling to the  $4s$  state is considerably weaker than the coupling to the  $3d$  state, the ionization signal follows the dye gain curve, except for frequencies near the  $4s$  resonance. On the low-energy side of the resonance, the ionization spectrum departs from following the dye gain curve and climbs more steeply upward until the ground state is resonant with the  $4s$  state. On the high-energy side of the resonance, the ionization drops sharply and again follows the dye gain curve. Floquet calculations show the ground Floquet state shifting towards the  $4s$  Floquet state on the low-energy side of the resonance and away on the high-energy side. Correspondingly, there is a sharp drop in the amount of  $4s$  character acquired by the ground Floquet state as the frequency is scanned through resonance with the  $4s$  state, resulting in the asymmetric resonance lineshape. Figure 5(b) shows the ionization spectrum as the laser frequency is scanned through resonance with the  $4d$  state. Because the  $2p$ - $4d$  oscillator strength is ten times stronger than the  $2p$ - $4s$  oscillator strength, Floquet calculations show that the ground Floquet state can acquire  $4d$  character at frequencies further off resonance. This fact is manifested in the ionization spectrum of Fig. 5(b) as a long tail on the low-energy side of the  $4d$  resonance. Again, the same argument can be made for connecting the ground Floquet state's acquisition of  $4d$  character with its energy shift; on the low-energy side of the resonance the shift is towards the  $4d$  Floquet state, while on the high-energy side the shift is away from the  $4d$  Floquet state.

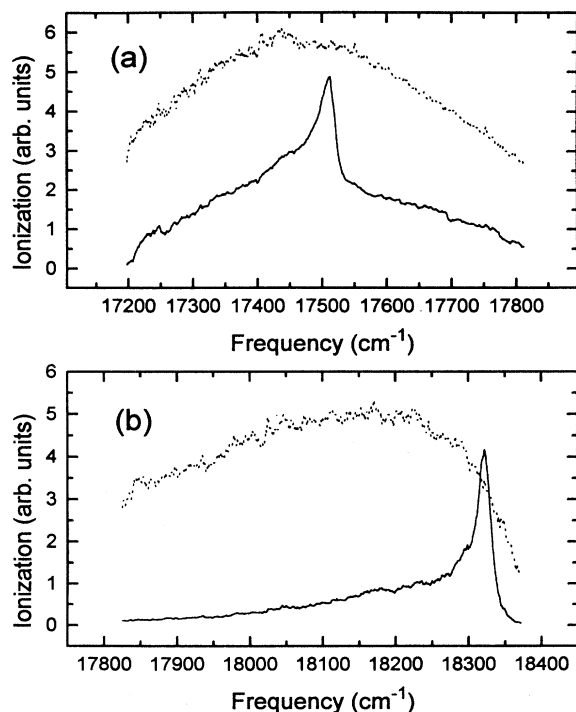


FIG. 5. (a) Total ionization as a function of laser frequency as the frequency is scanned through resonance with the  $4s$  state. Dotted trace is the dye gain curve of the ionizing laser. (b) Same as (a) for higher frequencies that bring the ground state in resonance with the  $4d$  state. Again, the dotted trace is the dye gain curve of the ionizing laser.

### B. The shift of the ground state

Figure 6 shows the shift of the ground state as a function of laser frequency. The crosses give the experimental data points, while the solid line represents a calculation based on the Floquet Hamiltonian. The experimental shift was found by taking the difference between the energy values corresponding to the front edge of the high and low intensity electron peaks for a specific laser frequency. The front edge of the electron peak corresponds to the highest-energy electrons that come from atoms at the center of the focus, where the ground state will experience the largest peak intensity, or equivalently, the largest ground-state shift. Although the shift at low intensities is very small, it is not zero. Thus the result gives the relative ac Stark shift produced by the peak laser intensity. There are also ponderomotive effects that influence the shift measurements. Because the electrons detected in this experiment have very low energies, they do not escape the focal region before the laser pulse turns off. As a result they do not regain the ponderomotive en-

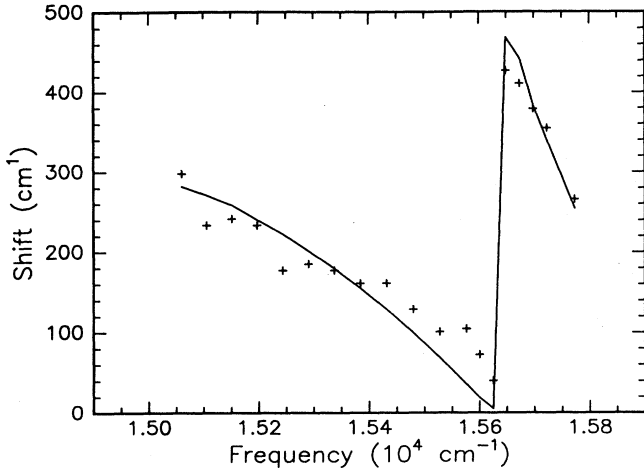


FIG. 6. Shift in energy of the ground Floquet state over the range of laser frequency for which Li is a strongly coupled three-level system. The crosses are the experimental values, while the solid line is the result of a Floquet calculation.

ergy that they lost at the moment of ionization due to the upward ponderomotive shift of the ionization limit. However, the ponderomotive energy at the maximum intensity reached in the experiment is approximately 17 meV, under 15% of the measured ground-state shift, so the ponderomotive effects are relatively small and do not obscure the general behavior of the ground-state shift as a function of laser frequency.

The data displayed in Fig. 6 can be explained using the Floquet picture mentioned earlier. For the frequency range in which the ground Floquet state lies between the  $2p$  and  $3d$  Floquet states, the data clearly show how the ground-state shift goes to zero as the ground Floquet state approaches degeneracy with the  $3d$  Floquet state. For frequencies where the ground Floquet state lies above both the  $2p$  and  $3d$  states, the effects of the couplings no longer counteract each other, and a relatively big shift is seen. The calculation was carried out by diagonalizing the Floquet Hamiltonian to obtain the energy eigenvalues of the ground Floquet state at both high and low laser intensity. The difference between these two eigenvalues gives the relative energy shift or the relative ac Stark shift of the ground Floquet state. The calculation includes the measured intensity profile of the laser as a function of laser frequency. The only adjustable parameter was the peak laser intensity, and this single adjustable parameter (which gave  $I_{\max} = 5 \times 10^{11} \text{ W/cm}^2$ ) was used for both the high and low intensity calculations, the difference of which gives the solid line seen in Fig. 6. The results of this Floquet analysis fit the experimental data quite well.

### C. Angular distributions and Floquet amplitude interference

The Floquet model of ionization described earlier does not include any interference effects. The total ionization signal depends on an incoherent summation of the excited-state amplitudes of the ground Floquet state.

Strictly speaking, this model of ionization is not correct, as it is possible for intermediate bound-state amplitudes to interfere with each other [9]. An instance in which bound state interference, an effect we have termed Floquet amplitude interference in this paper, *should* appear is in the angular distribution of the ionization signal. Angular distributions of ionization and ATI photoelectrons have been measured in alkali atoms (for example, see [10]) and are described by a sum of Legendre polynomials. We have found that describing our resultant angular distributions as a sum of spherical harmonics gives a more physically intuitive picture of the final-state continuum wave as follows.

Suppose the ground Floquet state of an atomic system when an ionizing laser is turned on is given by

$$\Psi_g = \sum \Phi_n = a_g \Phi_g + a_s \Phi_s + a_d \Phi_d, \quad (5)$$

where  $\Phi_g$  is the zero-field ground state, and  $\Phi_s$  and  $\Phi_d$  are zero-field  $s$  and  $d$  excited states that are bound by less than one photon. The  $s$  character of the ground Floquet state will ionize to a  $p$ -wave continuum state, while the  $d$  character can ionize to either a  $p$ - or  $f$ -wave continuum state. Calculations of the overlap between hydrogenic and continuum wave functions show that the probability of the  $d$  character ionizing to a  $p$  wave is two orders of magnitude smaller than the probability of ionizing to an  $f$  wave, so we neglect excitation of the  $p$  wave. The angular distribution of the ionization is then proportional to

$$\frac{d\sigma}{d\Omega} \propto |a_s r_{sp} Y_{10} + a_d r_{df} Y_{30}|^2, \quad (6)$$

where  $r_{sp}$  and  $r_{df}$  are radial matrix elements between the  $s$  ( $d$ ) excited states and the  $p$ - ( $f$ -) wave continuum states, and  $Y_{00}$  and  $Y_{20}$  are  $m=0$  spherical harmonics with  $l=1$  and  $l=3$ , respectively. Such an excitation produces an interference term resulting in a final state that is a coherent superposition of a  $p$  and  $f$  wave. This interference is weighted by the excited-state amplitudes of the ground Floquet state and the respective radial matrix elements.

Such an excitation is possible in Li if a laser is tuned so that the ground state plus two photons is in the vicinity of the  $4s$  and  $4d$  excited states. These two states are  $1611 \text{ cm}^{-1}$  apart and are shown in the energy-level diagram of Fig. 1. We have examined the evolution of the angular distribution as a function of frequency, and the results are shown in Fig. 7. With the ground Floquet state below or degenerate with the  $4s$  state, the angular distribution is a  $p$  wave; the ground Floquet state acquires a substantial amount of  $4s$  character, which is then ionized. However, placing the ground Floquet state  $25 \text{ cm}^{-1}$  above the  $4s$  state introduces new structure into the angular distribution. This structure is a result of the fact that the ground Floquet state has acquired some amount of  $4d$  character, in addition to  $4s$  character, with each character fraction ionized to an  $f$  and  $p$  wave, respectively. For bluer laser frequencies such that the ground Floquet state moves nearer to the  $4d$  state, the structure becomes even more apparent: the ground Floquet state acquires more  $4d$  character relative to  $4s$  character. With the ground Floquet state nearly degenerate with the  $4d$  state, the angu-

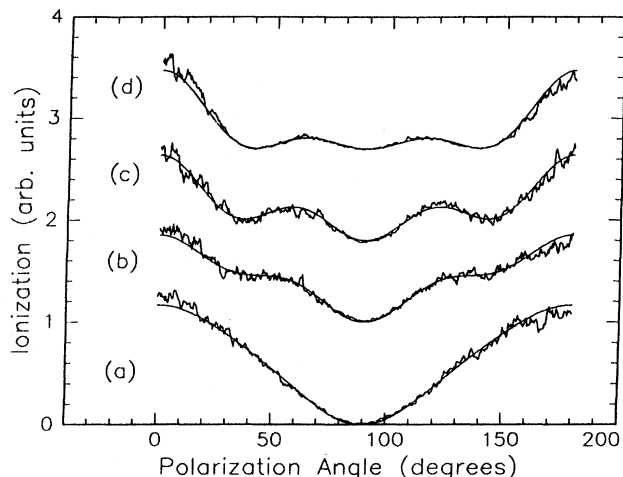


FIG. 7. Traces that show the evolution of the angular distribution of the ionization as the laser frequency is changed so that the ground Floquet state is (a) resonant with the  $4s$  state, (b)  $25\text{ cm}^{-1}$  above the  $4s$  state, (c)  $200\text{ cm}^{-1}$  above the  $4s$  state, (d) near resonance with the  $4d$  state ( $1554\text{ cm}^{-1}$  above the  $4s$  state). The solid line is a fit that consists of a linear combination of coherent and incoherent sums of  $p$  and  $f$  waves.

lar distribution has evolved into an  $f$  wave, only  $4d$  character is acquired and ionized.

It was argued earlier that when two excited-state fractions Floquet state are ionized simultaneously, the result is a coherent superposition of continuum waves. However, it was found that the angular distributions shown in Fig. 7 could not be fit to a coherent superposition of  $p$  and  $f$  waves. In fact, they could not be fit with an incoherent superposition, either; the solid lines in Fig. 7 are combinations of a coherent and incoherent superposition of  $p$  and  $f$  waves. How is this fact explained? It must be remembered that in a focused laser beam, the intensity spatially varies from being a maximum at the center of

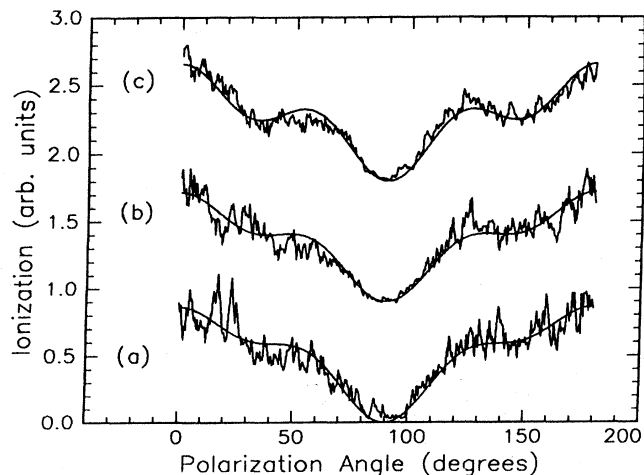


FIG. 8. Angular distributions of the ionization recorded at a laser frequency that places the ground Floquet state  $100\text{ cm}^{-1}$  above the  $4s$  state for the following relative intensities: (a)  $0.5I$ , (b)  $0.7I$ , (c)  $I$ .

the focus to zero at the edge of the focus. Therefore, different spatial regions (or equivalently, different intensity regions) will contain atoms having ground Floquet states with different relative amounts of  $4s$  and  $4d$  character. Ionization that originates from a constant intensity spatial region will be a coherent superposition of continuum waves. However, the signal that is recorded by the detector is the incoherent sum of all the different spatial regions.

The fact that the relative amounts of excited-state character acquired by the ground Floquet state is intensity dependent is shown by the results in Fig. 8. These angular distributions were recorded for a frequency that placed the ground Floquet state  $100\text{ cm}^{-1}$  above the  $4s$  state ( $1561\text{ cm}^{-1}$  below the  $4d$  state). The laser intensity was varied for each measurement with the top trace recorded at maximum laser intensity  $I$ , the middle trace at  $0.7I$ , and the bottom trace at  $0.5I$ . Again, the solid lines are fits that are linear combinations of coherent and incoherent sums of  $p$  and  $f$  waves. It is clear that the higher the intensity, the more the contribution from ionization of  $4d$  character is seen in the angular distribution. A higher intensity results in a larger shift of the ground Floquet state towards the  $4d$  state, allowing the ground state to acquire larger amounts of  $4d$  character. Previous experiments in the alkali atoms Na [11] and Cs [12] have observed intensity-dependent changes of angular distributions that were also attributed to intensity-dependent Stark shifts of atomic levels.

Unfortunately, the spatially varying intensity in the laser focus prevents one from using the experimental data to determine the relative amounts of the  $4s$  and  $4d$  character fractions in the ground Floquet state. However, the data do demonstrate that for laser frequencies below and on resonance with the  $4s$  state, the evolution of the ground Floquet state is largely adiabatic.

In addition to the ionization peak, a peak correspond-

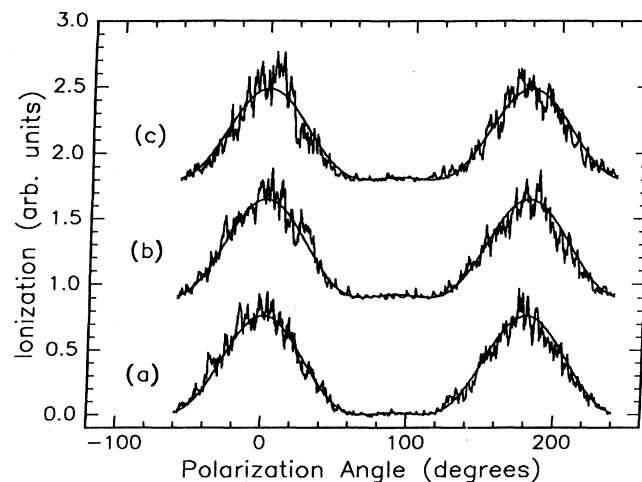


FIG. 9. Angular distributions of the first ATI peak for laser frequencies locating the ground Floquet state (a)  $25\text{ cm}^{-1}$  below the  $4s$  state (b) on resonance with the  $4s$  state, (c)  $25\text{ cm}^{-1}$  above the  $4s$  state. The solid line is a fit to a coherent sum of  $s$  and  $d$  waves.

ing to above-threshold ionization with one extra photon was observed in the electron spectra. Angular distribution of the ATI signal were taken at frequencies locating the ground state  $25 \text{ cm}^{-1}$  below, on resonance with, and  $25 \text{ cm}^{-1}$  above the  $4s$  state. At these frequencies, we know that the first step into the continuum is to a  $p$  wave. The ATI peak can then be either an  $s$  wave or a  $d$  wave. Because ATI is only produced by the high intensity region of the laser focus, there is no incoherent summation of different spatial regions. Indeed, the ATI angular distributions can be fit with a coherent superposition of  $s$  and  $d$  waves, as seen in Fig. 9. The fits are wave functions of the form  $|c_s Y_{00} + c_d Y_{20}|^2$ , where  $c_s$  and  $c_d$  are constants that determine the relative amounts of each continuum wave present in the final-state wave function. From these measurements, a value for the branching ratios for  $\Delta l = \pm 1$  transitions to the  $s$  and  $d$  continuum waves can be determined. A least-squares fit determined the ratio  $c_d/c_s$  to be 1.6 for each trace that is seen in Fig. 9.

Continuum-continuum transitions and the allowance for above-threshold photon absorption have been incorporated into a nonperturbative Floquet picture by Giusti-Suzor and Zoller [13]. They use a multichannel quantum-defect treatment (MQDT) [14] in which a set of dressed channels corresponding to different photon numbers is defined. Each channel is identified by the parameters  $\{N, l, m\}$  with  $N$  the Floquet, or photon, index and  $l, m$  the angular quantum numbers of the electron. Similar to the usual MQDT formulation, a reaction matrix is defined whose off-diagonal elements represent couplings between different channels. Once the channels are cou-

pled, the wave function of the electron may be expressed as a linear combination of channel wave functions, which are themselves a combination of the regular and irregular Coulomb functions multiplied by the appropriate spin and angular wave functions. The interference that is seen in the angular distributions of the ATI can be thought of as resulting from a coherent superposition of the dressed-channels identified by  $\{N, l, m\} = \{2, 0, 0\}$  and  $\{N, l, m\} = \{2, 2, 0\}$ .

## V. CONCLUSION

In conclusion, the Floquet theory offers a view of the multiphoton ionization process in which the evolution of the atomic states with the laser field can be calculated in a relatively easy manner. We have shown that a Floquet picture is useful in describing a variety of multiphoton measurements. Obvious advantages of this approach are the removal of the time dependence at the laser frequency and the ability to predict effects not foreseen by first-order perturbation theory. A Floquet analysis makes it clear how the energy shifts and the character evolution of bound intermediate states during the laser pulse are related, which in turn is paramount to understanding the ionization process. Although Floquet theory only allows for adiabatic evolution, coupled with the Landau-Zener level crossing theory a dynamical Floquet approach can be developed and used even for the case of diabatic evolution. As has been demonstrated recently, this dynamic Floquet approach is very useful in describing population transfer during the multiphoton ionization process [5,15].

- 
- [1] D. G. Papaioannou and T. F. Gallagher, Phys. Rev. Lett. **69**, 3161 (1992).
  - [2] P. Agostini and L. F. DiMauro, Phys. Rev. A **47**, R4573 (1993).
  - [3] R. B. Vrijen, J. H. Hoogenraad, H. G. Muller, and L. D. Noordam, Phys. Rev. Lett. **70**, 3016 (1993).
  - [4] J. G. Story, D. I. Duncan, and T. F. Gallagher, Phys. Rev. Lett. **70**, 3012 (1993).
  - [5] M. Edwards and C. W. Clark (unpublished).
  - [6] L. D. Landau, Phys. Z. Sowjetunion **2**, 46 (1932).
  - [7] C. Zener, Proc. R. Soc. London Ser. A **137**, 696 (1932).
  - [8] J. H. Shirley, Phys. Rev. B **138**, 979 (1965).
  - [9] J. Morellec, D. Normand, G. Mainfray, and C. Manus, Phys. Rev. Lett. **44**, 1394 (1980).
  - [10] Adila Dodhy, R. N. Compton, and J. A. D. Stockdale, Phys. Rev. Lett. **54**, 422 (1985); Phys. Rev. A **33**, 2167 (1986).
  - [11] W. Ohnesorge, F. Diedrich, G. Leuchs, D. S. Elliot, and H. Walther, Phys. Rev. A **29**, 1181 (1984).
  - [12] G. Petite, F. Fabre, P. Agostini, M. Crance, and M. Aymar, Phys. Rev. A **29**, 2677 (1984).
  - [13] A. Giusti-Suzor and P. Zoller, Phys. Rev. A **36**, 5178 (1987).
  - [14] M. J. Seaton, Rep. Prog. Phys. **46**, 167 (1983).
  - [15] J. G. Story, D. I. Duncan, and T. F. Gallagher, Phys. Rev. A **50**, 1607 (1994).